Earth Planets Space, **58**, 323–330, 2006

An empirical model of ionospheric *foE* over Wuhan

Xinan Yue[1,2,3], Weixing Wan[1], Libo Liu[1], and Baiqi Ning[1]

[1]*Institute of Geology and Geophysics, Chinese Academy of Sciences, Beijing 100029, China*
[2]*Wuhan Institute of Physics and Mathematics, Chinese Academy of Sciences, Wuhan 430071, China*
[3]*Graduate School of Chinese Academy of Sciences, Beijing, China*

(Received May 27, 2005; Revised August 22, 2005; Accepted September 21, 2005; Online published March 10, 2006)

Daytime half-hourly values of the critical frequency of the ionospheric E-layer, foE, obtained at Wuhan Ionospheric Observatory (geographic 114.4°E, 30.6°N; 45.2°dip), China, during the whole interval of 1957–1991 and 1999–2004 have been used to develop an empirical model. The model, including variations with local time, day number and solar cycle, is in agreement with the observations. A comparison between our model and IRI and Titheridge's model has also been made. Statistically, our model gives a better performance than IRI and Titheridge's model because data set is obtained with our own station. Both the IRI and Titheridge's model overestimate foE especially in May to September months. Combing with past investigations, we suggest that overestimation of ionospheric parameters by IRI may be a common feature in East Asia. This result is very helpful for both the correction of IRI in East Asia and the development of Chinese Reference Ionosphere (CRI) model.

Key words: Ionosphere, model, foE.

1. Introduction

Modeling of the ionospheric electron-density height profile Ne(h), as well as other parameters like the ion composition or electron and ion temperatures over the whole altitude range for all geographical positions, time spans, and geophysical conditions is an essential part of ionospheric physics and ionospheric space weather applications. A multitude of different ionospheric models including theoretical, empirical and semi-empirical model is available based on a variety of international and national organizations' modeling program. Many recent reviews have been published about ionospheric models. The most recent ones is proposed by Cander *et al.* (1999) and Bilitza (2002). Empirical models, which are established by statistical analysis of measured data, are widely investigated since they have the advantage of representing the ionosphere through actual measurements. Many local, regional and global empirical ionospheric models have been developed over the past years. The International Reference Ionosphere (IRI) is probably the most mature of these models, having undergone several decades of scrutiny and improvement.

The ionospheric E-layer has been studied for many years. The main features of the E-layer are well described by the simple Chapman theory. The physics involved is particularly simple for the E-layer, where the ionization time-constant is only a few minutes, so that conditions are always close to equilibrium. The ionospheric E-layer can provide relatively stable modes of propagation. So it is of great importance to predict the E-region parameters especially the critical frequency accurately and economically. The purpose of this paper is to obtain an empirical model of foE over Wuhan by using long time series of ionosonde data and also validate existed empirical models.

Many theoretical models (e.g., Buonsanto, 1990; Buonsanto *et al.*, 1992; Burns *et al.*, 1991; Titheridge, 1997; Mikhailov, 2003; Tan *et al.*, 2005) investigating the behavior of ionospheric E-layer have been developed over decades. However, most theoretical models give low NmE for daytime E-layer compared with measurements (Buonsanto *et al.*, 1992; Titheridge, 1997; Mikhailov, 2003). Contrarily, empirical models can predict the observations better because they are established on the basis of measurements. The prediction of E-layer critical frequency in most global empirical ionospheric models (e.g., IRI model) originates from a series of studies (Muggleton, 1971a, b, 1972a, b, 1975; Kouris and Muggleton, 1973a, b). They used foE data over a period of 11 years of many ionosonde stations all over the world to obtain the dependence of foE on latitude, season, solar flux and local time. The final empirical equation was described in detail by Muggleton (1975). Many researchers compared ionosonde data which were not used in the IRI model with the corresponding IRI-predicted values. Most comparisons show that there was a good agreement between the observed and predicted foE (or NmE) values. However, daytime values of NmE calculated by IRI model show some unexpected variations with latitude and season because of abrupt changes in the empirical equations or extrapolation of the equations into regions with little experimental data (Titheridge, 2000). Titheridge (1996, 1997, 2000) introduced a global E-layer peak model on the calculations with a full time-varying model. His model result gives a smooth variation and agrees well with experimental data. In addition, this model can help us to study the

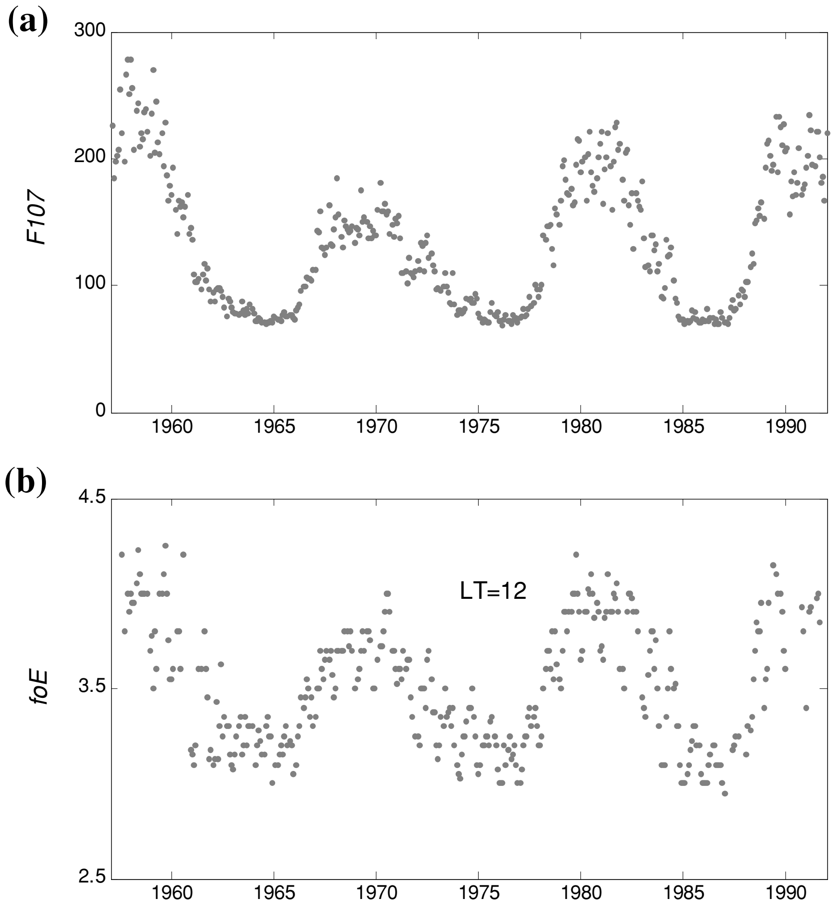

Fig. 1. (a) Monthly median $F107$ index during the whole internal of 1957–1991. (b) Monthly median foE of local noon time during the interval of 1957–1991.

E-layer's morphology when and where there is little data available, such as at night or over the ocean.

There were also many local and regional ionospheric models related to the E-layer critical frequency. Zolesi *et al.* (1993) developed a regional ionospheric model by using Fourier analysis on the monthly median values of ionospheric characteristics including foE from seven ionospheric stations in Europe. Holt and Zhang (2002) constructed a detailed empirical model of ionospheric E- and F-region over Millstone Hill. McKinnel and Poole (2003) established a local E-layer critical frequency model over Grahamstown, South Africa, by using neural networks. In this paper we construct an empirical foE model over Wuhan. Though there are many empirical ionospheric model related to E-layer available, it is of great importance for us to do this work for several reasons as follows. (1) Since 1957, ionosonde measurements have been routinely made at Wuhan Ionospheric Observatory, which located in central China, is just away from the northern crest of equatorial anomaly in East Asia. Based on long time series of ionospheric parameters over Wuhan, Liu *et al.* (2004) constructed single-station models of $foF2$ using Fourier expansion and cubic-B splines approaches. Chen *et al.* (2004) developed a simple method to model electron density profile. So, an empirical ionospheric foE model may be an important complement to the local empirical ionospheric model over Wuhan. (2) The original IRI model does not include ionosonde data over China. Many Chinese researchers have compared ionosonde data observed over China with predicted values by IRI and most results showed not very good agreement. Wu *et al.* (1996) developed a revised regional model called the Chinese Reference Ionosphere (CRI) and it is more accurate than the IRI for use in and around China. However the CRI did not modify the E-layer critical frequency and the data used by CRI did not include the ionosonde data of Wuhan. So modeling the ionospheric foE over Wuhan may be useful for the development of the CRI model. (3) Bilitza (2001) had indicated that developing models for the variability of ionospheric parameters is very useful and important. An accurate prediction of foE over Wuhan may be a very important base of this work.

The remainder of this paper is organized as follows. Section 2 describes the data source that used in the present investigation. The model is introduced in Section 3. We give our model results and comparison with other empirical models in Section 4 and conclusions in Section 5.

2. Data Source

Since the International Geographical Year (IGY, 1957) the routinely operated ionosonde 5830 which was made in Hungary has been run over Wuhan (geographic 114.4°E, 30.6°N; 45.2°dip) for more than thirty years and it was replaced by digisonde 256 in 1991. The data used in this

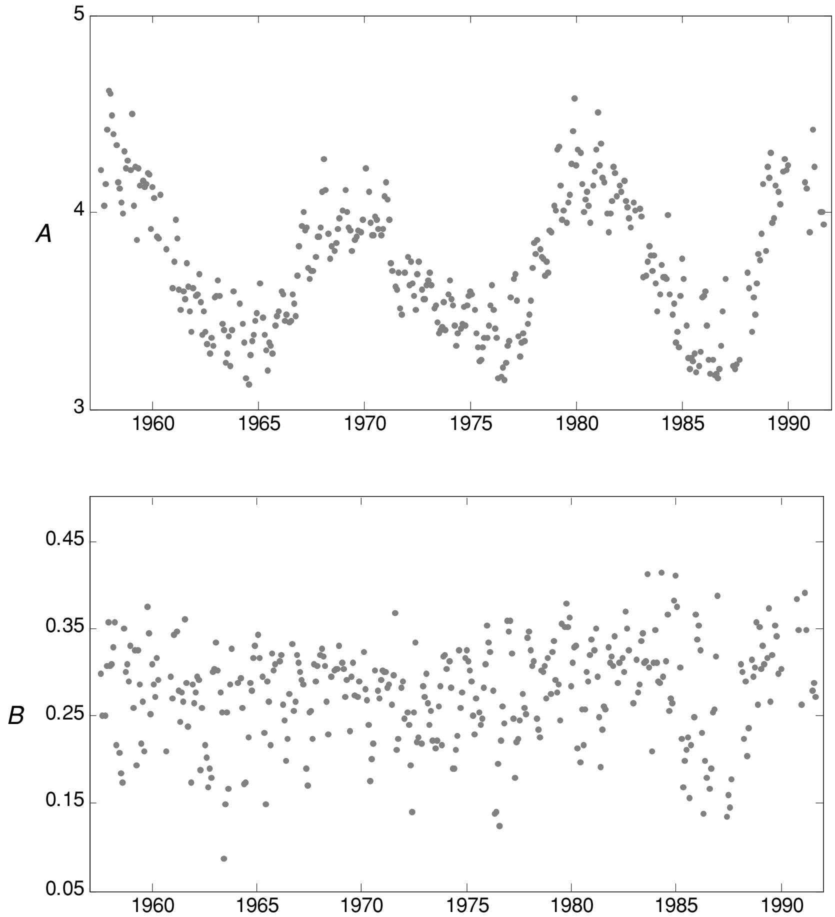

Fig. 2. (a) Parameter A in Eq. (7) fitted by least-squares method during the interval of 1957–1991. (b) Parameter B in Eq. (7) fitted by least-squares method during the interval of 1957–1991.

work is the E-layer critical frequency (foE) scaled from the observed ionosonde records during the interval of 1957–1991 and 1999–2004.

It is known that foE uncertainties are greatest during nighttime because electron densities are quite low and only a few reliable measurements exist. So we only use the daytime foE data. The data near sunrise and sunset will also be eliminated because reflection traces in ionogram are mostly distorted by horizontal gradients in the ionosphere near sunrise and sunset. To avoid the influence resulted from occasional mistakes in daily observation and investigate the average behavior of E-layer, we use the monthly median patterns of the chosen data.

In general terms, daytime (between 8 and 16 hours in local time in this work) half-hourly values of monthly median foE during the period of 1957–1991 and 1999–2004 are used to construct the model. The corresponding monthly median $F107$ are also used to represent solar activity level. Figure 1(a) displays monthly median $F107$ during 1957–1991. Figure 1(b) shows monthly median foE of local noon time during 1957–1991. A high correlation can be observed between these two parameters by comparing Fig. 1.

3. Method Description

The variation with the solar zenith angle of the critical frequency of the E-layer, foE, under the premise of the balance of electron production and loss rate, satisfies the equation:

$$foE = A(\cos\chi)^{0.25} \tag{1}$$

where A is determined by electron production rate and loss rate. Many investigators assume a relation of the type $foE \propto (\cos\chi)^n$ and find the value of n is bigger than 0.25 for a number of stations (Muggleton, 1972b) by linear regression method. As we know, atmospheric temperatures increase rapidly with height in the daytime E-region. This brings on an increase in the scale height $H = \mathrm{kT/mg}$ and a decrease in production rate. Including this effect gives (Rishbeth and Garriott, 1969)

$$foE = A(\cos\chi)^{0.25(1+g)} \tag{2}$$

where $g = dH/dh$ is the scale height gradient. Titheridge (2000) calculated the average value of scale height gradient which is 0.2 by the values of scale height derived from MSIS86 model between the height of 105 and 110 km. The same value was also obtained by empirical modeling (Muggleton, 1972b). In our empirical modeling we assume the relation between foE and $\cos\chi$ as follows:

$$foE = A(\cos\chi)^{B} \tag{3}$$

However, all the above equations are applicable only when solar zenith angle is not big. When χ is near 90°, as near

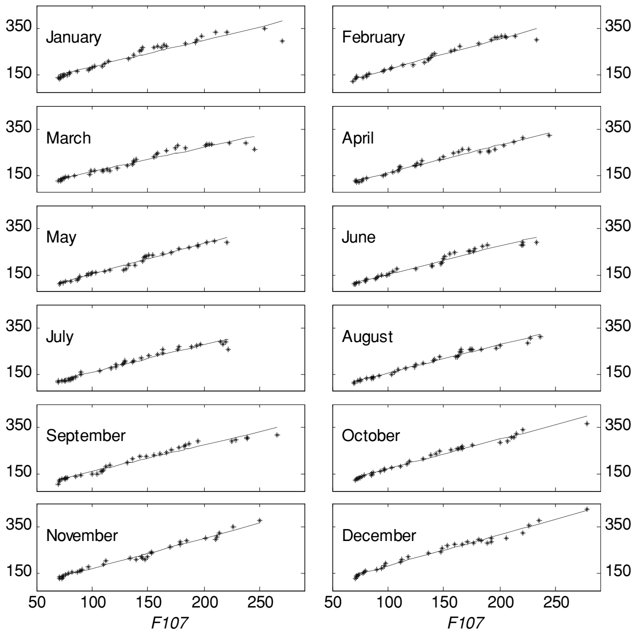

Fig. 3. The relation between A4 and $F107$ index month by month during the interval of 1957–1991 and 1999–2004, where A is the parameter fitted by Eq. (7). Solid dots show the fitted A by observed foE data and solid lines represent the linear fits between A4 and $F107$.

sunrise and sunset, the "plane earth" approximation is not good enough. The factor $\sec\chi$ varies along the path of the radiation and can no longer be taken outside the optical depth integration. Chapman defined a "grazing incidence function" called Chapman function to overcome this difficulty. We should replace $\cos\chi$ by Chapman function ($CH(H,\chi)$) when zenith angle is large. But it is difficult to calculate the value of Chapman function because it is a rather complex function and H varies with χ in a manner difficult to define. So, several approximative formulas to the Chapman function are developed by different researchers (Muggleton, 1972a; Titheridge, 1988; Rawer and Bilitza, 1990). As different formulas have no distinctions for daytime conditions according to our study, we apply the approximative formula developed by Rawer and Bilitza (1990) which is also used by IRI. The formula is given by:

$$CH(H,\chi) = \sec(\chi + \delta_x) \quad (4)$$

where $\delta_\chi = -3\ln(1 + e^{(\chi-89.98)/3})$. By adding δ_χ to χ in Eq. (5), we get the equation:

$$foE = A(\cos(\chi + \delta_\chi))^B \quad (5)$$

Figure 2 displays parameters A and B in Eq. (5) obtained by least-squares fit method from 1957 to 1991 over Wuhan. Parameters A and B during the interval of 1999–2004 are not plotted here. To get precise estimation of A and B, there are several principles we should follow when processing the data: (1) Monthly median patterns of the data is adopted. The data whose median counts are not bigger than 10 is excluded to ensure the quality. (2) Data are limited between local time 8 and 16 hours to eliminate undue data near sunrise and sunset. (3) Only the month which has more than 8 valid data points is adopted (There should have 17 data points at most between local time 8 and 16 hours in monthly median patterns of half-hourly data for every month).

As can be seen in Fig. 2, A has an obvious solar cycle variation while B does not. There is also no regular seasonal variation of B in our research. Kouris and Muggleton (1973a) used foE data over a period of 11 years from 45 ionospheric stations to investigate the diurnal exponent parameter p in equation: $(foE)^4 = q(\cos\chi)^p$, where $p = 4B$. Their studies showed that the value of p does not vary significantly in non-equatorial latitudes and the average value of p is 1.20. The result has been used in IRI (Bilitza, 1990). Constant value of diurnal exponent parameter was also adopted by Titheridge (2000) in his global empirical E-layer peak model. To simplify the form of our empirical model, we also use a constant value of B. We get the best estimation of B over Wuhan by using our own ionosonde data. We set B between 0.20 and 0.35 with a step of 0.001. For each of the B value, we calculate total relative deviation:

$$\delta foE = \sum \mathrm{abs}(foE_{\mathrm{obs}} - foE_{\mathrm{reg}})/foE_{\mathrm{obs}} \quad (6)$$

where foE_{obs} is observed value and foE_{reg} is the regression value for fixed value of B. Then the best estimation of B, 0.286, is determined by a judgment which gives the smallest δfoE. It is a little smaller than the fixed value used by IRI. This maybe resulted from that we have assumed constant value of normalized foE for a given day. It is coincident with the conclusion of Titheridge (2000) that values of N_0 are most nearly constant when using a slightly smaller index p in the equation $N_0 = \mathrm{NmE}/(\cos\chi)^p$.

Comparing Fig. 2(a) and Fig. 1(a), there is a highly correlated relationship between parameter A and $F107$. The relationship between foE and solar activity has been investigated by many researchers. Muggleton (1971b) found a worldwide relationship $\mathrm{NmE} \propto (foE)^2 \propto (1+0.00334R)$ through linear regression analysis for 15 ionosonde stations all over the world during the period 1949–1959. Titheridge (1997) found that mid-latitude values of NmE are closely proportional to $(F107 + 40)^{0.5}$ in all seasons. The above two conclusions are identical because $F107$ is proportional to $(R + c)^2$ where R is sunspot number and c is a constant. So we can assume $foE \propto m(F107 + n)^{0.25}$ in the study. The depending of foE on solar activity is mainly contributed by parameter A in Eq. (5). Figure 3 illustrates the solar activity variations of quartic values of A for every month. Solid lines represent the linear fit: $A^4 = p+qF107$. We can conclude from the figure that there is a good linear relationship between A^4 and $F107$ for most months in Wuhan station.

Besides the solar activity, parameter A in Eq. (5) also has a distinct variation with solar zenith angle of local noon time (Kouris and Muggleton, 1973b). Figure 4 displays seasonal variation of A and $\cos\chi_{\mathrm{noon}}$ of the 15th day of every month separately. Average A of every month is plotted with error bars against month. There is a highly correlation between A and $\cos\chi_{\mathrm{noon}}$ as indicated in the figure. The relationship between A and $\cos\chi_{\mathrm{noon}}$ can be represented as $A \propto (\cos\chi_{\mathrm{noon}})^p$, where p is negative (Kouris and Muggleton, 1973b). According to empirical model IRI, p should be equal to-0.0693 for Wuhan station. But by the method

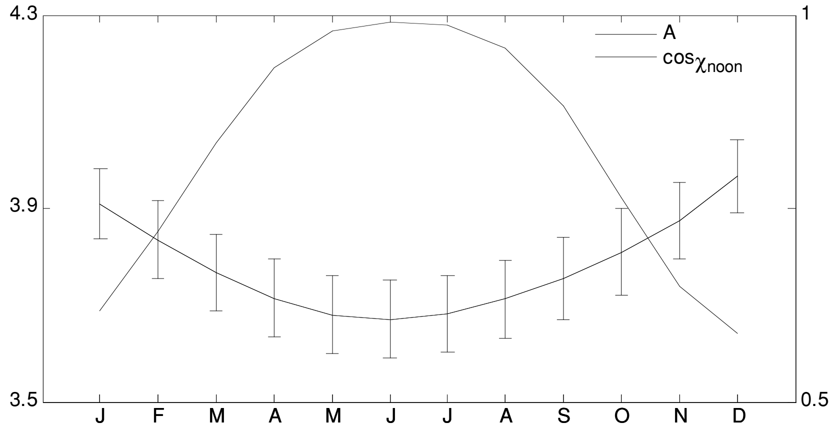

Fig. 4. Seasonal variation of parameter A fitted by Eq. (7) and the cosine of local noon time solar zenith angle ($\cos\chi_{noon}$). Average A of every month is plotted with error bars against month. Broken line show $\cos\chi_{noon}$ of the 15th day of every month.

of least-squares to the distribution of the data points (A, $\cos\chi_{noon}$) for every month from 1957 to 1991 and 1999–2004, we find that the best estimation of p is-0.0513 over Wuhan, which is a little different from that in IRI.

From the discussion above, we know that parameter A can be represented by the equation:

$$A = m(n + F107)^{0.25}(\cos\chi_{noon})^p \quad (7)$$

The dependence of foE on solar activity and solar zenith angle has been investigated in detail in the description above. According to Eqs. (5) and (7), foE can be generally expressed as

$$foE = m(n + F107)^{0.25}(\cos\chi_{noon})^p(\cos(\chi + \delta_\chi))^B \quad (8)$$

where $F107$ is the solar activity index, $\cos\chi_{noon}$ is the cosine of local noon time solar zenith angle, and χ is the solar zenith angle. M and n are the coefficients used to determine the relationship between foE and $F107$. δ_χ is the adjustment to χ which are required to describe the dependence of foE on solar zenith angle well. We have indicated that the best estimation of p is-0.0513 and B is 0.286 over Wuhan. By using the monthly median values of foE observed in Wuhan and $F107$ index during the whole interval of 1957–1991 and 1999–2004, we can get the best estimation of parameter m and n in Eq. (8) with least-squares fit method, which is 1.058 and 25.23 respectively. Thus we obtain a local empirical foE model.

4. Comparison with IRI and Titheridge's Model

We have introduced an empirical foE model at Wuhan ionosonde station. Virtually it is developed by using the same mathematical description as IRI. But the coefficients are different from that used in IRI because they are derived from the observation. We make a comparison in this part for the predicted foE between our model and IRI and also with that of Titheridge's model that was introduced in Section 1.

Figure 5(a) illustrates sample values of the observed (stars) and modeled (lines) foE. The left panels of the picture are for our simple model, middle for the IRI model, and right for the Titheridge's model. Years for high solar activity (1959, 2002), low solar activity (1966), the descending part of solar cycle (1973) and the ascending part of solar cycle (1978) were chosen. We should point out that the parameters in our model have no difference whether the foE data in five chosen years is included or not. It is indicated from the figure that all the three models can fit the observations very well for the chosen years.

To reveal the performance of three models accurately over Wuhan, we also plot the error distributions and the corresponding standard deviations in Fig. 5(b). Panels from top to bottom are for years of 1959, 1966, 1973, 1978 and 2002 respectively. The error distributions and the corresponding standard deviations during the whole interval of 1957–1991 and 1999–2004 in given months are demonstrated in Fig. 6. Variation of standard deviations of relative deviations of model values from observations between local time of 8 and 16 hours is illustrated in Fig. 7.

When validating the performance of three models in predicting foE over Wuhan which has been illustrated in Figs. 5(a) to 7, several points should be discussed.

Statistically, our single-station model gives a better performance than the IRI and Titheridge's model. As shown in Fig. 5(b) and 6, its standard deviations lie around 0.05 to 0.08 MHz. In contrast, the IRI and Titheridge's model have a lower accuracy with standard deviations of about 0.06 to 0.11 MHz and 0.07 to 0.12 MHz separately. This is understood because of the limitation of global empirical models and rather complicated nature of the ionosphere. Besides, IRI does not include Chinese data, and this will result in no good agreement between observed and predicted values in China (Huang *et al.*, 1995; Wu *et al.*, 1996). Titheridge's model has a relatively larger difference than ours. This may be due to the fact that his model is based on theoretical results while ours on observations. Taking no account of our model, IRI provides the better agreement with the observation than Titheridge's model. It should be stressed that all the three models neglected the Sq current effect, which is the main reason that deviation can not be reduced further.

The error distributions of the IRI and Titheridge's model shift to the positive side especially in months from May to September as illustrated in Fig. 6. The possible reason may be that both models describe seasonal variation of foE not precisely when applied to Wuhan. It shows that both IRI

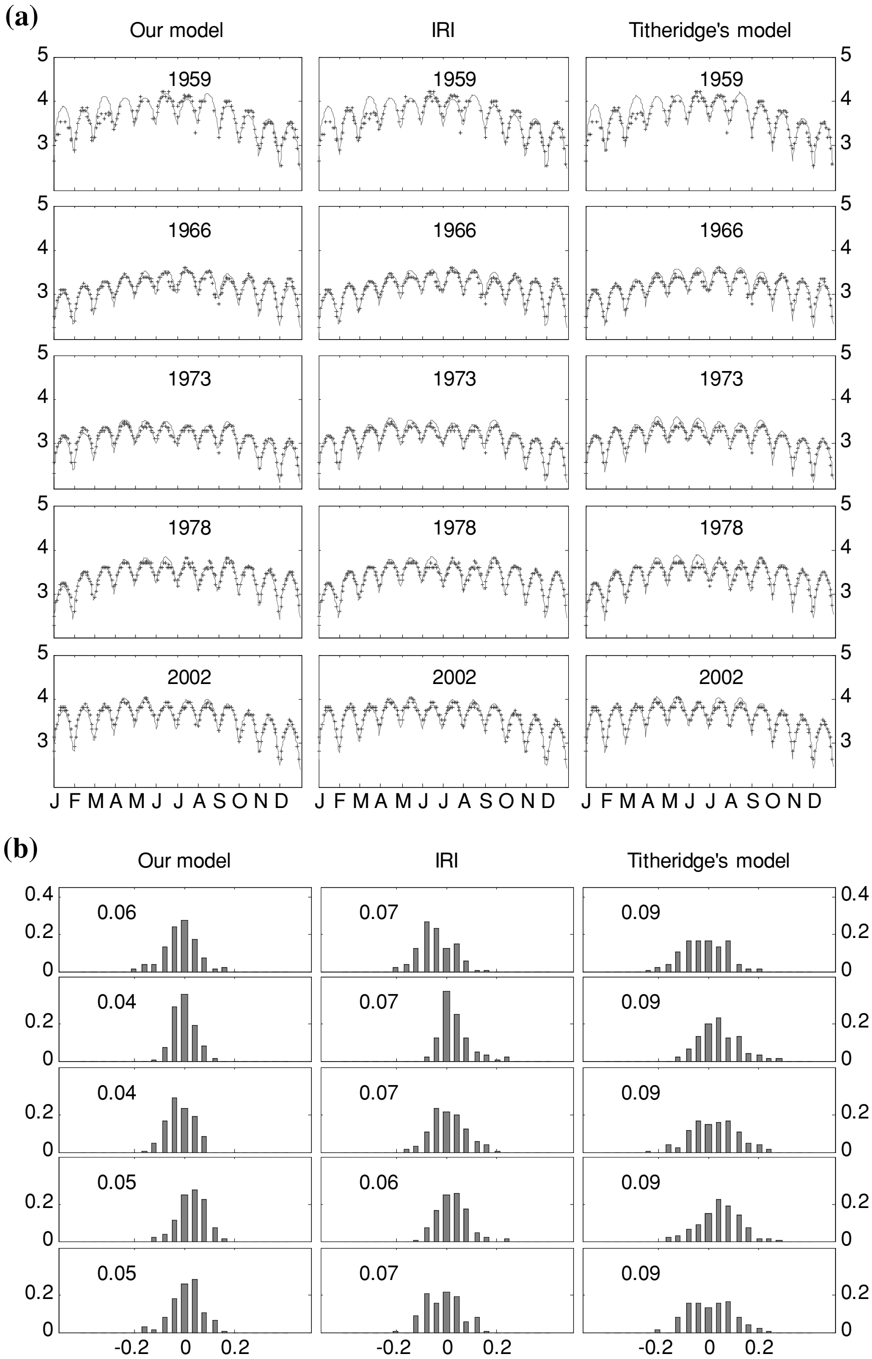

Fig. 5. (a) Observed (star dots) and modeled (lines) foE for high solar activity (1959, 2002), low solar activity (1966), the descending part of solar cycle (1973), and the ascending part of solar cycle (1978) are plotted against month. The values of foE are in monthly median patterns between local time 8 and 16 hours. (b) Same as Fig. 5(a), but for the error distributions. The standard deviations are presented in the upper left-hand corner of each subplot.

and Titheridge's model overestimate foE over Wuhan. The interesting thing is that the IRI model also overestimates TEC (Chen *et al.*, 2002) and $foF2$ (Liu *et al.*, 2004) over Wuhan. We think it is not an occasional coincidence, but relate to the characteristics of regional ionosphere of Wuhan which located away from the northern crest of equatorial anomaly in East Asia. Luo *et al.* (1994) also found that the bottom-side values of the electron density predicted by IRI are bigger than the values obtained from four Chinese ionosonde stations. It seems that overestimation of ionospheric parameters by IRI is a common feature in East Asia.

Considering diurnal variations of standard deviations of relative deviations of model values from observations illustrated in Fig. 7, all the three models have a maximum standard deviation in local noon time and a minimum in the morning and afternoon. According to the model results of Titheridge (2000), the parameter N_0 should vary throughout the day, where N_0 is the normalized peak density in equation: $\text{NmE} = N_0 C_\chi^{0.6}$. However, both IRI and our model assume a constant value for normalized peak density in a given day. This may be the primary reason that the standard deviations have a marked diurnal variation for IRI and our

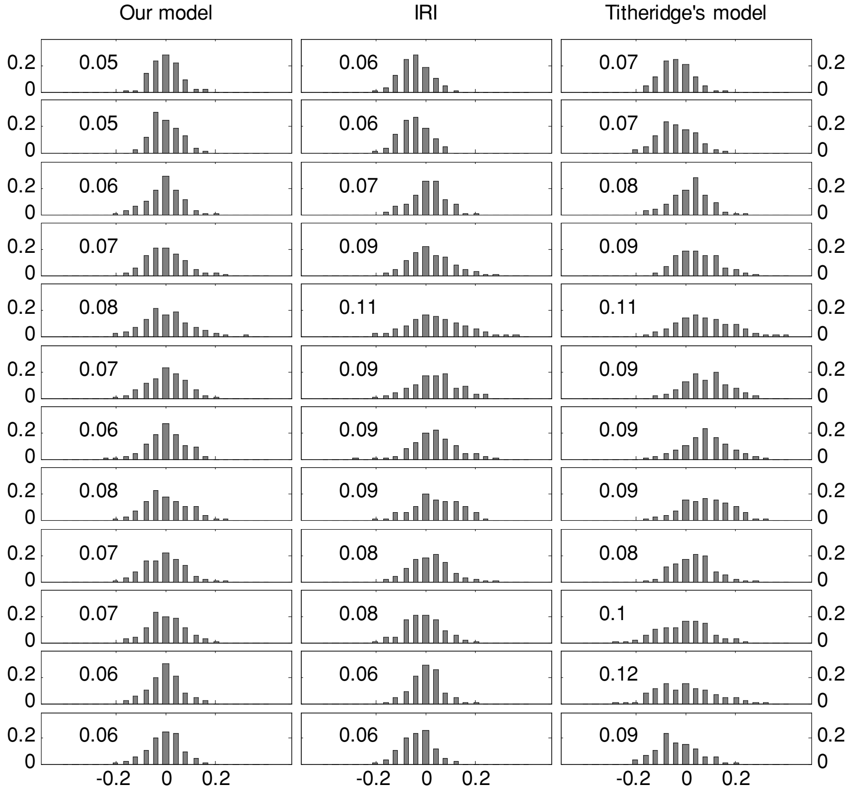

Fig. 6. The distributions and standard deviations of three model errors over Wuhan during the internal of 1957–1991 and 1999–2004 in months. Panels from top to bottom are for months from January to December respectively. The number in each subplot represents the standard deviations of model errors in corresponding month.

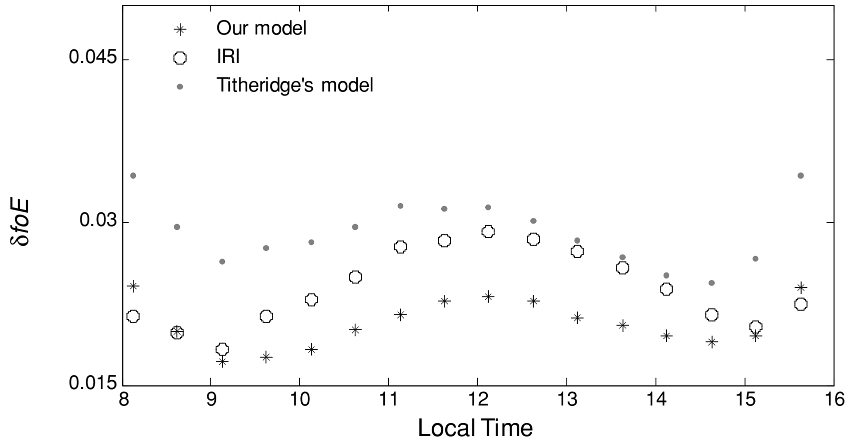

Fig. 7. Diurnal variation of standard deviations of relative deviations of model values from observations for our model (star dots), IRI (open circles) and Titheridge's model (solid dots) during the internal of 1957–1991 and 1999–2004 over Wuhan.

models. But different from the Titheridge's model, both IRI and our models have a bigger standard deviation in the afternoon than in the morning. This may relate to the linear approximation to N_0 with a gradient used by Titheridge's model (Titheridge, 2000). But why the standard deviations of Titheridge's model also have marked diurnal variation need further investigation.

5. Summary

We have developed an empirical ionospheric foE model as an important complement to the local empirical ionospheric model over Wuhan using the ionosonde measurements during the whole interval of 1957–1991 and 1999–2004. The model incorporates local time, day number and solar cycle variations of foE. We have also made a comparison between our model and IRI and Titheridge's model. The results show that the standard deviations of our model lie around 0.05 to 0.08 MHz, while the IRI and Titheridge's model have a lower accuracy with standard deviations of about 0.06 to 0.11 MHz and 0.07 to 0.12 MHz, respectively. Since our model is constructed based on our own observation, it is expected to give better prediction performance than IRI and Titheridge's model. Our model, IRI and Titheridge's model have a marked diurnal variation in the standard deviations between relative deviations of model values and observations over Wuhan. We suggest that an accurate description of the diurnal variation of normalized electron density and takeing into account the Sq effect may be useful if we want to reduce the standard deviation further.

Both IRI and the Titheridge's model overestimate foE over Wuhan especially in months from May to September. Combining with the conclusion that IRI also overestimates $foF2$ (Liu *et al.*, 2004) and TEC (Chen *et al.*, 2002) over Wuhan, we think that it is not an occasional coincidence, but related to the characteristics of regional ionosphere of Wuhan which located away from the northern crest of equatorial anomaly in East Asia. Luo *et al.* (1994) also found that the bottom-side values of the electron density predicted by IRI are bigger than the values obtained from four Chinese ionosonde stations. It seems that overestimation of ionospheric parameters by IRI is a common feature in East Asia.

Our model can meet the need of precise prediction especially in the propagation modes. It is not only an important complement to the local empirical ionospheric model over Wuhan but also very helpful in the development of regional ionospheric model of China, CRI. We recommend that the phenomena of overestimation should be paid attention to when apply IRI and Titheridge's model to East Asia region.

Acknowledgments. This work is supported by the KIP Pilot Project (kzcx3-sw-144) of CAS, National Science Foundation of China (40134020), and National important Basic Research Project (G2000078407). The IRI model code was provided by the National Space Science Data Center (NSSDC) ftp://nssdcftp.gsfc.nasa.gov. The $F107$ indices are downloaded from the SPIDR web site http://spidr.ngdc.noaa.gov/. The authors thank Titheridge J. E. for providing global E-layer peak model and warm-hearted help.

References

Bilitza, D., International Reference Ionosphere 1990, Report 90-22, National Space Data Center, World Data Center A for Rockets and Satellites, Code 930.2, Goddard Space Flight Center, 1990.

Bilitza, D., International Reference Ionosphere 2000, *Radio Sci.*, **36**(2), 261–275, 2001.

Bilitza, D., Ionospheric models for radio propagation studies, in *The Review of Radio Science 1999–2002*, edited by W. R. Stone, pp. 625–679, IEEE Press, Piscataway, N. J, 2002.

Buonsanto, M. J., A study of the daytime E-F1 region ionosphere at midlatitudes, *J. Geophys. Res.*, **95**(A6), 7735–7747, 1990.

Buonsanto, M. J., S. C. Solomon, and W. K. Tobiska, Comparison of measured and modeled solar EUV flux and its effect on the E-F1 region ionosphere, *J. Geophys. Res.*, **97**(A7), 10513–10524, 1992.

Burns, C. J., E. Turunen, H. Matveinen, H. Ranta, and J. K. Hargreaves, Chemical modeling of the quiet summer D- and E-regions using EISCAT electron density profiles, *J. Atmos. Terr. Phys.*, **53**, 115–134, 1991.

Cander, L. R., R. Leitinger, and M. F. Levy, Ionospheric models including the auroral environment, in Workshop on Space Weather, Report WPP-155, Noordwijk, The Netherlands, European Space Agency (ISSN 1022-6656), 135–142, 1999.

Chen, Y., W. Wan, L. Liu, and L. Li, A statistical TEC model based on the observation at Wuhan Ionospheric Observatory, *Chin. J. Space Sci.*, **22**(1), 27–35, 2002.

Chen, Y., W. Wan, L. Liu, and T. Mao, A simple method of modeling electron density profile using ionospheric parameters, *Chin. J. Space Sci.*, **24**(3), 194–202, 2004.

Holt, J. M. and S. R. Zhang, A local empirical model of the E and F region ionosphere based on 30 years of Millstone Hill incoherent scatter data, AGU Fall Meeting 2002, SA21A-0425, 2002.

Huang, X., Y. Su, and K. Zhang, Ionospheric structure and profile over Wuchang, China, *Adv. Space Res.*, **15**(2), 149–152, 1995.

Kouris, S. S. and L. M. Muggleton, Diurnal variation in the E-layer ionization, *J. Atmos. Terr. Phys.*, **35**, 133–139, 1973a.

Kouris, S. S. and L. M. Muggleton, World morphology of the Appleton E-layer seasonal anomaly, *J. Atmos. Terr. Phys.*, **35**, 141–451, 1973b.

Liu, L., W. Wan, and B. Ning, Statistical modeling of ionospheric foF2 over Wuhan, *Radio Sci.*, **39**, RS2013, doi:10.1029/2003RS003005, 2004.

Luo, F., K. Dai, and K. Quan, A comparison of the International Reference Ionosphere (IRI-90) with the electron density profile of the ionosphere observed in China, *Chin. J. Space Sci.*, **14**(4), 305–311, 1994.

McKinnel, L. A. and A. W. V. Poole, A neural network based electron density model for the E layer, *Adv. Space Res.*, **31**(3), 586–595, 2003.

Mikhailov, A. V., Model results for the midlatitude daytime E region: EUV ionization rate and α (NO+) relationship, *Int. J. Geomagn. Aeron.*, **4**(1), 47–55, 2003.

Muggleton, L. M., Appleton's last note on the E-region seasonal anomaly, *J. Atmos. Terr. Phys.*, **33**, 1291–1297, 1971a.

Muggleton, L. M., Solar cycle control of Nm(E), *J. Atmos. Terr. Phys.*, **33**, 1307–1310, 1971b.

Muggleton, L. M., A describing function of the diurnal variation of Nm(E) for solar zenith angles from 0 to 90°, *J. Atmos. Terr. Phys.*, **34**, 1379–1384, 1972a.

Muggleton, L. M., Regression-line studies of E-region seasonal anomaly, *J. Atmos. Terr. Phys.*, **34**, 1985–1391, 1972b.

Muggleton, L. M., A method of predicting foE at any time and place, *Telecommunications Journal*, **42**, 413–418, 1975.

Rawer, K. and D. Bilitza, International reference ionosphere-plasma densities: status 1988, *Adv. Space Res.*, **10**(8), 5–14, 1990.

Rishbeth, H. and O. K. Garriott, *Introduction to Ionospheric Physics*, Academic Press, New York and London, 1969.

Tan, H., W. Wan, J. Lei, L. Liu, and B. Ning, A theoretic model for the mid-latitude ionospheric E layer, *Chin. J. Geophys.*, **48**(2), 243–251, 2005.

Titheridge, J. E., An approximate form for the Chapman grazing incidence function, *J. Atmos. Terr. Phys.*, **50**, 699–701, 1988.

Titheridge, J. E., A direct allowance for the effect of photoelectrons in ionospheric modeling, *J. Geophys. Res.*, **101**, 357–369, 1996.

Titheridge, J. E., Model results for the ionospheric E region: solar and seasonal changes, *Ann. Geophys.*, **15**, 63–78, 1997.

Titheridge, J. E., Modelling the peak of the ionospheric E-layer, *J. Atmos. Solar-Terr. Phys.*, **62**, 93–114, 2000.

Wu, J., K. Quan, K. Dai, F. Luo, X. Sun, Z. Li, C. Cao, R. Liu, and C. Shen, Progress in the study of the Chinese reference ionosphere, *Adv. Space Res.*, **18**(6), 187–190, 1996.

Zolesi, B., L. R. Cander, and G. De Franceschi, Simplified ionospheric regional model for telecommunication applications, *Radio Sci.*, **28**(4), 603–612, 1993.

X. Yue, W. Wan (e-mail: wanw@mail.igcas.ac.cn), L. Liu, and B. Ning